

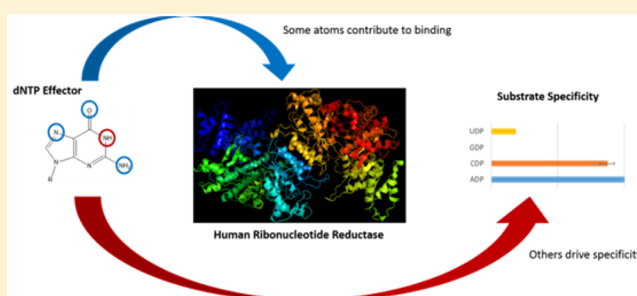
Nucleoside Analogue Triphosphates Allosterically Regulate Human Ribonucleotide Reductase and Identify Chemical Determinants That Drive Substrate Specificity

Andrew J. Knappenberger,[†] Md. Faiz Ahmad,[‡] Rajesh Viswanathan,[§] Chris G. Dealwis,[‡] and Michael E. Harris^{*,†}

[†]Departments of Biochemistry, [‡]Pharmacology, and [§]Chemistry, Case Western Reserve University, Cleveland, Ohio 44106, United States

Supporting Information

ABSTRACT: Class I ribonucleotide reductase (RR) maintains balanced pools of deoxyribonucleotide substrates for DNA replication by converting ribonucleoside diphosphates (NDPs) to 2'-deoxyribonucleoside diphosphates (dNDPs). Binding of deoxynucleoside triphosphate (dNTP) effectors (ATP/dATP, dGTP, and dTTP) modulates the specificity of class I RR for CDP, UDP, ADP, and GDP substrates. Crystal structures of bacterial and eukaryotic RRs show that dNTP effectors and NDP substrates bind on either side of a flexible nine-amino acid loop (loop 2). Interactions with the effector nucleobase alter loop 2 geometry, resulting in changes in specificity among the four NDP substrates of RR. However, the functional groups proposed to drive specificity remain untested. Here, we use deoxynucleoside analogue triphosphates to determine the nucleobase functional groups that drive human RR (hRR) specificity. The results demonstrate that the 5-methyl, O4, and N3 groups of dTTP contribute to specificity for GDP. The O6 and protonated N1 of dGTP direct specificity for ADP. In contrast, the unprotonated N1 of adenosine is the primary determinant of ATP/dATP-directed specificity for CDP. Structural models from X-ray crystallography of eukaryotic RR suggest that the side chain of D287 in loop 2 is involved in binding of dGTP and dTTP, but not dATP/ATP. This feature is consistent with experimental results showing that a D287A mutant of hRR is deficient in allosteric regulation by dGTP and dTTP, but not ATP/dATP. Together, these data define the effector functional groups that are the drivers of human RR specificity and provide constraints for evaluating models of allosteric regulation.



Regulation by allostery is a fundamental property of proteins and of enzymes in particular.¹ Enzymes acting as key control points in metabolism are typically under tight allosteric regulation;² therefore, functional insights into the nature of protein allostery can provide a better understanding of biology as well as design principles for therapeutic development. Decades of research beginning with inquiries into the structure and function of hemoglobin have revealed numerous examples of allostery, and mechanisms of site-to-site communication have been thoroughly explored in many systems.^{3–5} Providing experimental constraints useful for developing and benchmarking models of protein allostery remains an important challenge in biochemistry. Ribonucleotide reductases (RRs) present a key example of enzyme regulation by allostery in which additional mechanistic detail at a chemical level would be highly valuable to both biology and biomedicine.

RRs make up a ubiquitous and highly conserved class of enzymes that catalyze the reduction of ribonucleotides to produce 2'-deoxyribonucleotides. RR is essential for DNA synthesis and deoxynucleotide pool maintenance, and the activity of various RRs is tightly regulated at the levels of

transcription, localization, and allostery.^{6–12} The total enzymatic activity of class I RR and its specificity among the four NDP substrates are under tight allosteric control by nucleoside and deoxynucleoside triphosphate effectors.⁶ ATP and dATP regulate total activity through binding at the Activity site (A-site). In eukaryotic class Ia RRs, this association results in the formation of active or inactive hexamers of RR.^{13–20} Binding of dNTP effectors to the Specificity site (S-site) of class I RR modulates the relative k_{cat}/K_m for ADP, CDP, GDP, and UDP at the Catalytic site (C-site) (Figure 1A). A general model in which ATP/dATP binding directs reduction of CDP and UDP, dGTP directs reduction of ADP, and dTTP directs reduction of GDP is well-supported by biochemical and structural data.^{6,7,10,12,20–22} However, key information about the precise workings of RR allostery is still lacking. Areas in which open questions still exist include the role of specific protein–ligand interactions in altering RR structure and a description of the

Received: June 12, 2016

Revised: September 9, 2016

Published: September 16, 2016

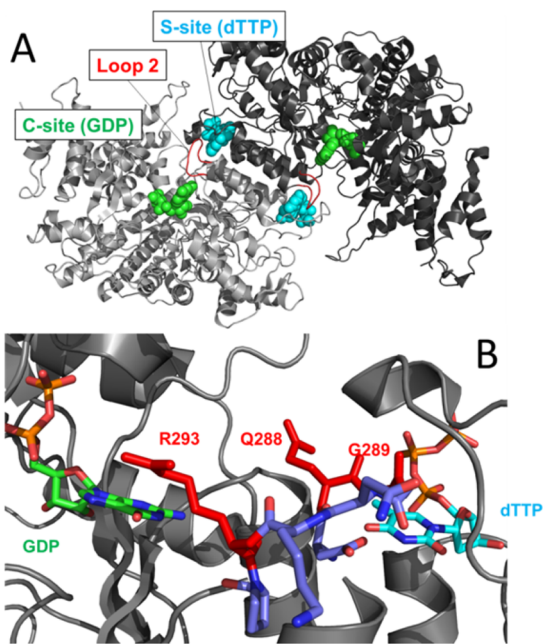


Figure 1. Structure of human ribonucleotide reductase and location of the S-site and C-site (PDB entry 3HND, 3.21 Å resolution). (A) Three-dimensional structure of the large subunit dimer of hRR. The polypeptide backbone is colored gray with loop 2 colored red. The locations of the S-site, C-site, and loop 2 are indicated. dTTP is bound in the S-site, and GDP is bound in the C-site. (B) Detail of the S-site, loop 2, and C-site motif involved in allosteric regulation. Effector (dTTP, blue sticks) binding alters the loop 2 conformation (dark blue sticks) to determine the optimal substrate (GDP, green sticks) in the C-site. Loop 2 amino acids are shown as dark blue sticks with the conserved residues Q288, G289, and R293 shown as red sticks. Q288 and R293 have been implicated in substrate recognition through *in vitro* and *in vivo* studies (see the text). G289 is also well-conserved and likely adds additional flexibility to loop 2, though its role has not been tested via structure–function studies. In this structural model, R293 forms an indirect contact with the phosphate groups of the NDP substrate (GDP).

energetic coupling among effector binding, protein conformational changes, and the resulting effects on substrate discrimination.

Recent high-resolution crystal structure models of the large subunits of human RR (hRR), *Saccharomyces cerevisiae* RR (ScRR), *Thermotoga maritima* RR (TmRR), and *Escherichia coli* RR (EcRR) provide key insights into how allosteric communication is accomplished. They highlight the importance of a flexible nine-amino acid region called loop 2 that forms part of both the C-site and the S-site^{7,10,12,20} (Figure 1A). For both bacterial and eukaryotic class I RRs, binding of dNTP effectors to the S-site biases the conformational distribution of loop 2 such that it presents a binding pocket with more favorable potential interactions for a particular NDP substrate in the C-site (Figure 1B). Amino acids in loop 2 that are proximal to the effector nucleobase are conserved at positions Q288, G289, and R293 (hRR numbering), consistent with a central role in allosteric communication (Figure 2A). Residues G295 and A296 are also conserved and may play a more structural role involving loop flexibility. Several residues, including Y285, D287, and K292, are also conserved in eukaryotic RR enzymes and are variable between eukaryotes and bacteria. The pattern of substrate specificity and regulation by effector binding is highly similar among bacterial and

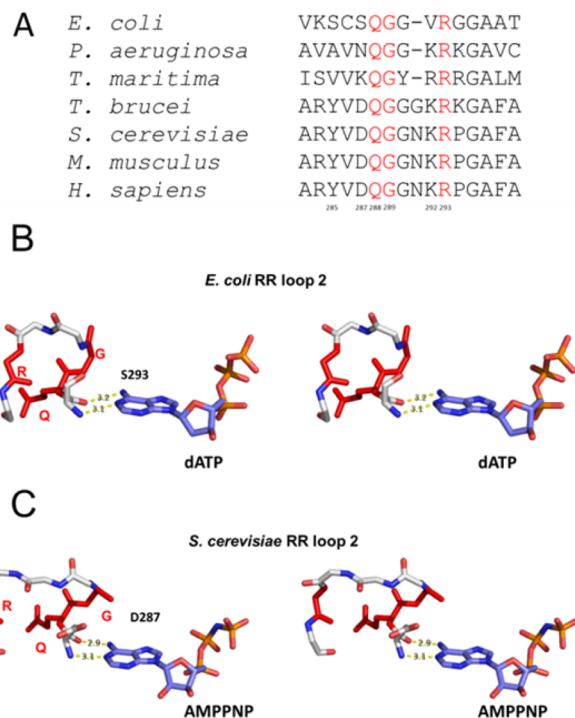


Figure 2. Comparison of RR loop 2 across species. (A) Sequence alignment of the loop 2 region of RRs discussed in this study.^{7,10,12,20,43,55,56} Positions 288, 289, and 293 (human numbering) are colored red. Positions 288, 289, and 293 are fully conserved within this sample, while considerable variation exists at position 287. hRR has an aspartic acid residue at position 287, and mutation of D287 to alanine severely restricts the ability of hRR to modulate its specificity in response to effector binding (Figure 9). (B) Crystal structure of EcRR bound to dATP and CDP (not shown) (PDB entry 5CNS, 2.97 Å resolution).¹⁰ (C) Crystal structure of ScRR bound to AMPPPNP and CDP (not shown) (PDB entry 2CVU, 2.9 Å resolution).⁷ In panels B and C, the S-site ligand is shown as dark blue sticks. Loop 2 amino acids are shown as white sticks, with the conserved glycine, glutamine, and arginine residues shown as red sticks. Key contacts described in the original references are shown.

eukaryotic RRs (Figure S1), consistent with common mechanisms of allosteric communication among these enzymes.

Because of recent advances in RR structural biology and limited structure–function studies, the roles of conserved residues as well as the potential consequences of phylogenetic sequence variation in loop 2 are now coming into focus. The available X-ray crystal structures of class I and II RRs show that the effector nucleobase functional groups form contacts with the N-terminal amino acids of loop 2. Structural models of both *T. maritima* and *E. coli* RR suggest that N1 and N6 of dATP are hydrogen-bonded to the main chain amide and carbonyl groups of the same homologous residue in both enzymes [K202 in TmRR (PDB entry 1XJM) and S293 in EcRR (PDB entry 5CNS)]¹⁰ (Figure 2B). Similar interactions between ScRR and ATP are inferred from data obtained in the presence of AMPPPNP (PDB entry 2CVU).⁷ The use of AMPPPNP as an analogue of ATP/dATP has the potential to produce adventitious interactions and binding modes that are not representative of those that occur between the enzyme and native effector *in vivo*. In spite of this, the ScRR structural model remains valuable for our studies of the biomedically important human enzyme because it depicts a eukaryotic RR in complex with an S-site ligand that is similar to the native ATP/

dATP. This model shows that the adenine N1 and N6 atoms also contact the main chain amide and carbonyl of the same homologous position (D287 in hRR). The overall geometry of loop 2, including the positions of conserved residues, appears to be similar to the model of EcRR (Figure 2C). However, the relative importance of adenosine functional groups in stabilizing the appropriate conformation of loop 2 is not known.

The model of allosteric regulation by dGTP and dTTP is less clear, although some common features can be observed. N1 and N2 of dGTP appear to direct specificity for ADP in both the TmRR model (PDB entry 1XJK)¹² and the EcRR structure (PDB entry 5CNU)¹⁰ by interacting with backbone functional groups. However, dGTP contacts the same K202 position as ATP in the TmRR structure, while in EcRR, dGTP contacts the universally conserved Q294 (PDB entry 5CNU) (Q288 in hRR). In contrast, O6 of dGTP contacts the main chain amide groups of G289 and G290 and N1 hydrogen bonds to the side chain of D287 (PDB entry 2CVX) in ScRR. As a consequence, the loop geometries and positions of conserved residues are distinct between the bacterial and eukaryotic RR models of the dGTP- and ADP-bound forms (Figure S2A,B). A similar situation is observed for dTTP, which makes minimal contacts with loop 2 in the *T. maritima* RR structural model (PDB entry 1XJJ). In the EcRR structure, the nucleobase N3 atom contacts the backbone carbonyl of C292, altering contacts involving Q294 (PDB entry 5CNV). The dTTP nucleobase contacts residues outside loop 2 in models of ScRR and hRR. This allows a more compact geometry (PDB entry 2CVW) compared to that of the bacterial enzyme (Figure S2C,D).

The available structural models make it clear that non-covalent interactions between the effector nucleobase and the N-terminal side of loop 2 are likely to contribute to allosteric communication. However, there is still significant ambiguity regarding the chemical features of the effector that drive specificity and the interactions that stabilize the appropriate loop 2 conformations. Importantly, our current understanding of the interactions between loop 2 and the dNTP effector in the biomedically important human enzyme remains comparatively limited. Determining the precise contributions of effector functional groups to substrate specificity is essential for evaluating any model of RR allosteric regulation. Therefore, we systematically tested the ability of a series of deoxynucleoside triphosphate analogues to allosterically regulate hRR specificity. The results identify the primary nucleobase functional groups that direct hRR specificity for its four native NDP substrates. This new information provides experimental support for current structural models of effector recognition by eukaryotic class I RR. Achieving a detailed chemical picture of RR regulation by nucleotide binding also contributes to a more complete understanding of protein allostery in general. Although this study is directed at understanding basic principles of RR regulation, because altered nucleotide pools inhibit cell growth, insight into the chemical basis for RR specificity is potentially useful for the development of artificial effectors with therapeutic applications.

■ EXPERIMENTAL PROCEDURES

Purification of Human and Yeast Ribonucleotide Reductases. The two human RR subunits hRRM1 and hRRM2 were purified according to procedures described by Fairman et al.²⁰ Briefly, hRRM1 was recombinantly expressed in BL-21 (DE3) RIL *E. coli* cells, while hRRM2 was expressed in BL-21 (DE3) *E. coli* cells. hRRM1 was purified via peptide

affinity chromatography. The wild-type hRR specific activity across all substrates in the presence of 50 μM dTTP was $0.0066 \pm 0.00052 \text{ mol s}^{-1} (\text{mol of hRRM1})^{-1}$.²⁰ The specific activity across all substrates in the presence of 50 μM dGTP was $0.0055 \pm 0.0017 \text{ mol s}^{-1} (\text{mol of hRRM1})^{-1}$.²⁰ hRRM2 was purified by addition of an N-terminal six-His tag and subsequent Ni-NTA affinity chromatography. The hRRM2 subunit was assembled into the active cofactor via iron loading under anoxic conditions using ferrous ammonium sulfate. The two RR subunits from *S. cerevisiae*, ScRR1 and ScRR2R4, were purified by a method similar to that used for hRRM1 and hRRM2 except that ScRR1 was recombinantly expressed in BL-21 (DE3) pLysS *E. coli* cells and purified to homogeneity using peptide affinity chromatography. The specific activity for ScRR across all substrates in the presence of 1 mM ATP was $0.11 \pm 0.017 \text{ mol s}^{-1} (\text{mol of ScRR1})^{-1}$.²⁰ Similar values were obtained when ATP was present in the presence or absence of dGTP or dTTP. After one freeze–thaw cycle, active ScRR2R4 still contained $\sim 0.15 Y^{\bullet}/\beta\beta'$ (0.15 tyrosyl radical per small subunit heterodimer) (data not shown).

In Vitro Measurement of Ribonucleotide Reductase Multiple-Turnover Kinetics. Kinetic assays were conducted at 37 °C in 50 mM gly-gly (pH 7.7), 15 mM MgCl₂, and 20 mM DTT. Reaction mixtures used to validate internal competition kinetics as shown in Figure 3 contained 0.5 μM R1, 5 μM R2, 1 mM ATP, and 0.75 mM dGTP. Substrates ADP and CDP were present at concentrations that range from 300 μM to 3 mM. Prior to the start of the reaction, all components except R1 were mixed in 250 μL of reaction buffer and incubated for 2 min at 37 °C. Two 30 μL aliquots were removed prior to initiating the reaction. These samples were used to measure the substrate concentrations and verify the efficacy of subsequent boronate chromatography. The reactions were started by adding hRRM1, and aliquots were removed at specific times after mixing (2–30 min) and the reactions quenched (see below). Reaction times were chosen to permit $^{\prime}k$ (relative $k_{\text{cat}}/K_{\text{M}}$) measurements for slow substrates while maintaining product accumulation in the linear phase of the reaction under steady-state conditions (<10% reacted).

Upon removal, all aliquots were quenched by being rapidly cooled to –80 °C. Substrate and product concentrations were quantified by UV absorbance, as described below. Measuring substrate and product concentrations independently permits greater precision in $^{\prime}k$ (relative $k_{\text{cat}}/K_{\text{M}}$) measurements and allows for confirmation that steady-state assumptions are satisfied. Accumulation of product concentration as a function of time yielded the observed velocity (v_{obs}) for each substrate. Relative velocity is measured via product accumulation rather than substrate depletion because of the small fraction of reaction in experimental aliquots. Substrate concentration and v_{obs} data were combined via eq 1^{30,36–38} (see below) to yield $^{\prime}k$, or the ratio of each substrate's $k_{\text{cat}}/K_{\text{M}}$ relative to that of the reference substrate. hRRM2 or ScRR2R4 was added in 10-fold excess over hRRM1 or ScRR1.

$$\frac{v_{\text{obs}1}}{v_{\text{obs,ref}}} = \left[\frac{(k_{\text{cat}}/K_{\text{M}})_1}{(k_{\text{cat}}/K_{\text{M}})_{\text{ref}}} \right] \frac{[S_1]}{[S_{\text{ref}}]} = ^{\prime}k_1 \frac{[S_1]}{[S_{\text{ref}}]} \quad (1)$$

Quantification of Ribonucleotide Reductase Substrate Specificity by Internal Competition. Experiments measuring native hRR and ScRR specificity were performed essentially as described above. Mixtures for ATP experiments contained 1 mM ATP as the only allosteric effector. Mixtures

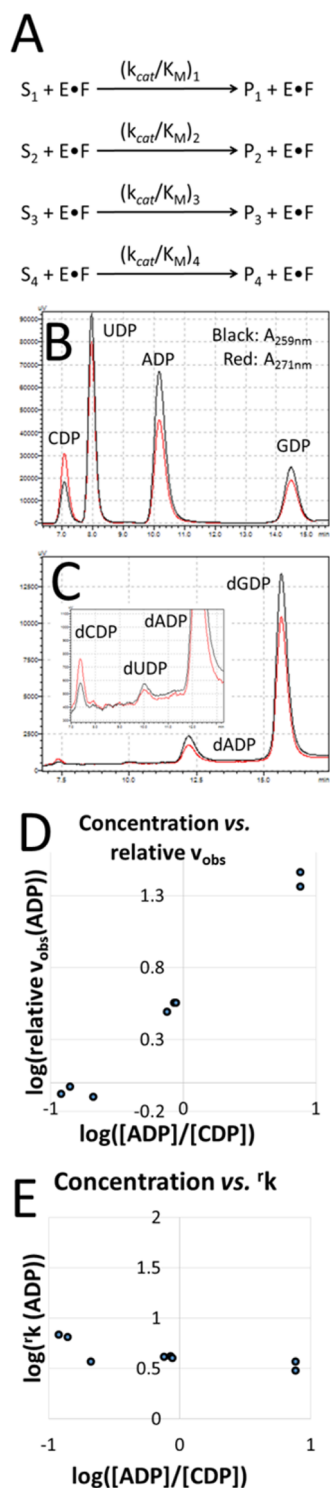


Figure 3. Application of internal competition to measurement of hRR specificity. (A) Simplified kinetic scheme showing reaction of substrate (S) with the enzyme–effector complex (E·F) to produce product (P). Substrate S_n reacts with second-order rate constant $(k_{cat}/K_M)_n$ to produce P_n . (B) Representative chromatogram of a $t = 0$ aliquot from an assay of hRR specificity containing all four NDP substrates. This aliquot experienced all aspects of experimental workup except boronate chromatography, so substrate NDPs are present. (C) Representative chromatogram of a $t = 30$ min aliquot with substrates removed by boronate chromatography, showing only dNDP products. The inset shows details of the region of the chromatogram containing dCDP, dUDP, and dADP. (D) Plot of the observed reaction velocity (v_{obs}) vs $[S_1]/[S_2]$. Each symbol represents one independent trial. (E)

Figure 3. continued

Data from panel D were used to calculate the relative k_{cat}/K_M ($^r k$) using eq 1 with ADP as the experimental substrate and CDP as the reference. The calculated value is plotted as a function of $[S_1]/[S_2]$ that was measured directly for each reaction by integration of the NDP peaks from the $t = 0$ chromatogram as shown in panel A.

for dGTP experiments also contained 0.75 mM dGTP, and mixtures for dTTP experiments also contained 1.6 mM dTTP. These concentrations ensure that ATP is excluded from the S-site.^{15,23} Substrates ADP, CDP, GDP, and UDP were present at concentrations ranging from 50 μ M to 1.5 mM. Typically, substrates were present at 0.5 mM. However, substrates with high $^r k$ values were given concentrations as low as 50 μ M, and substrates with low $^r k$ values were given concentrations as high as 1.5 mM to facilitate v_{obs} measurement.

Quantitative analysis of the specificity induced by deoxynucleotide analogues was performed essentially as described above. All deoxynucleotide analogues were purchased from TriLink at stock concentrations of 100 mM in H_2O . ATP (1 mM) was omitted to prevent competition with effectors of interest. Substrates were present at equimolar concentrations (0.6 mM). In experiments with pyrimidine analogues, ADP was omitted to prevent adventitious binding of ATP present as a minor contaminant. Nucleoside triphosphate effector analogues were present at the concentrations indicated in the text. All nucleotide effector analogues tested were present at a concentration of 100 μ M. This concentration is \sim 100-fold greater than the dissociation constants for the natural effectors dGTP and dTTP and stimulated enzymatic activity for all analogues except dCTP derivatives (Figure 5).²³ Measurement of the apparent dissociation constant between hRRM1 and dTTP in the presence of 50 μ M 2-aminopurine-drTP or dITP was performed by varying the concentration of dTTP and measuring the $^r k$ value for GDP with all four NDP substrates present at 600 μ M (Figure 8C). Measurement of the dissociation constant between hRRM1 and dTTP was performed by measuring the specific GDP reductase activity in the presence of 1.2 mM GDP, no other NDP substrates, and varying concentrations of dTTP (Figure 8B).

Reaction mixtures of RR substrates and products were processed according to procedures described by Hendricks et al.²⁴ Briefly, frozen aliquots were thawed by addition of 169.4 μ L of boronate chromatography buffer [150 mM ammonium acetate and 15 mM $MgCl_2$ (pH 9)] and 1 M $MgCl_2$ to a final $MgCl_2$ concentration of 18 mM. For experiments described in Figure 8B, 1 μ L of dATP was added as an internal standard. Diluted aliquots were immediately processed by application to a tuberculin syringe packed with >250 μ L of Affi-Gel 601 (Bio-Rad). Aliquots were pushed through the syringe at a flow rate of \sim 1 mL/min. The resin was then washed with 400 μ L of boronate chromatography buffer at the same flow rate. The resulting mixture was acidified with \sim 5 μ L of 85% phosphoric acid to pH 3; 100 μ L was immediately injected onto a Phenomenex SphereClone anion exchange column with 150 mM sodium phosphate (pH 3.7) as the mobile phase. Analytes were eluted via a gradient of 150 to 800 mM sodium phosphate (pH 3.7) on a Shimadzu LC 20-AB chromatograph. The chromatograph's dual-wavelength detector was set to 259 and 271 nm. Peaks were identified by comparing their retention times and A_{259}/A_{271} values with those of standards. ADP, GDP, and UDP were quantified by their A_{259} ; CDP was quantified by

its A_{271} . A final aliquot was treated identically but not subjected to boronate chromatography, so that the concentration of each substrate in the reaction mixture could be measured in a manner independent of the expected concentration.

Site-Directed Mutagenesis of Human Ribonucleotide Reductase. Site-directed mutagenesis of hRRM1 was conducted using the Thermo Phusion Site-Directed Mutagenesis Kit. The D287A mutant was generated using primers 5'-ACAGCTAGATATGTGGCTCAAGGTGGGAACAAG-3' and 5'-GTTGTTATATACTCTCAGCATCGGTACAAGGC-3'. Plasmid DNA was purified using the QIAGEN Miniprep and Midiprep plasmid purification kits. Plasmid sequences were verified by Sanger sequencing from primers 5'-TTCGGCTT-TAAGACGCTAGA-3', 5'-CTTGGCATTTAGACATCTT-TGA-3', 5'-TTGGCTGAAGTCACTAAAGTCG-3', 5'-CGC-AGAGTCTTGTCAGGAGA-3', and the T7 promoter. D287A hR1 was purified via the same method as wild-type hR1. The specific activity for D287A hRR in the presence of 1 mM ATP was $0.053 \pm 0.002 \text{ mol s}^{-1} (\text{mol of hRRM1})^{-1}$, in the presence of 50 μM dGTP $0.0028 \pm 0.00048 \text{ mol s}^{-1} (\text{mol of hRRM1})^{-1}$, and in the presence of 50 μM dTTP $0.0072 \pm 0.0025 \text{ mol s}^{-1} (\text{mol of hRRM1})^{-1}$.

Sequence Alignment. Amino acid sequence alignment was performed using the Multiple Sequence Alignment feature of Clustal Omega.^{25,26} cDNA sequences of the ribonucleotide reductase large subunit were retrieved from GenBank.²⁷

RESULTS

Quantification of the NDP Substrate Specificity of Yeast and Human RR by Internal Competition. RR is intrinsically a multisubstrate enzyme. Thus, a means for determining the rate constants for all four NDP substrates is required to dissect mechanisms of allosteric regulation. Relatively few studies comprehensively interrogate RR specificity, because of the technical difficulties and low throughput of single-substrate assays.^{15,28} Internal competition is an alternative method for quantifying enzyme rate constants that involves analyzing the change in the ratios of concentrations of alternative substrates or products as a function of reaction progress in reaction mixtures containing multiple substrates.^{29–32} This approach has potential advantages over direct fitting of kinetic data by offering higher precision, increased throughput, and less sensitivity to variation in enzyme specific activity.^{29,30} Internal competition kinetics have been used extensively to measure kinetic isotope effects,^{32,33} and substrate and product ratios have been measured using a wide range of analytical methods. Importantly, Mathews and colleagues demonstrated simultaneous quantification of RR reduction of all four NDP substrates using boronate chromatography to remove unreacted ribonucleotides followed by separation of dNDP products using ion exchange high-performance liquid chromatography (HPLC).²⁴ This method has been used previously to investigate RR enzymology and permits direct, sensitive, and quantitative comparison of the effects of different allosteric effectors on specificity using internal competition kinetics.

As shown in Figure 3A, a single RR enzyme can combine with one of four NDP substrates and react to form dNDP products. Thus, multiple substrate enzymatic reactions of this kind follow internal competition kinetics in which differences in observed reaction rates reflect differences in $k_{\text{cat}}/K_{\text{m}}$ for individual NDP substrates.^{34,35} Under steady-state conditions, the reaction velocity for a given substrate relative to a reference

substrate should be proportional to the relative concentrations of the two substrates and their relative specificity constant or ' k ' (eq 1).

Therefore, quantification of the distribution of dNDP products in RR reaction mixtures containing all four NDP substrates in steady-state reactions permits the relative $k_{\text{cat}}/K_{\text{m}}$ for each substrate to be calculated. To validate this approach for hRR, we tested whether changes in the concentrations of two NDPs ($[S_1]/[S_{\text{ref}}]$) affect the observed ' k ' values. We assayed hRR in the presence of varied concentrations of substrates ADP and CDP (0.3 mM ADP and 3 mM CDP, 1.8 mM ADP and 1.8 mM CDP, or 3 mM ADP and 0.3 mM CDP) and effectors ATP and dGTP at concentrations of 1 and 0.75 mM, respectively (Figure 3D,E). Product accumulation and the initial substrate concentrations were quantified directly by anion exchange HPLC, providing increased precision in the calculated ' k ' values and ensuring that experimental reaction mixtures remained within steady-state conditions. The results show that $v_{\text{obsADP}}/v_{\text{obsCDP}}$ is proportional to $[\text{ADP}]/[\text{CDP}]$ and that the calculated relative specificity constant, ' k_{ADP} ', varies <2-fold over the 100-fold range of substrate concentrations examined.

To provide a baseline for comparison of the effects of nucleoside analogue triphosphates on allosteric regulation, we first quantified the specificity of hRR and ScRR bound to one of the three native allosteric effectors (ATP, dGTP, or dTTP) included in the reaction mixture at a concentration of 1, 0.75, or 1.6 mM, respectively (Figure 4). Consistent with amino acid sequence conservation in loop 2, the two species' enzymes have highly similar specificity.^{7,20} The substrate specificity directed by the three native nucleotide effectors is not absolute; each effector state will accept multiple substrates, albeit over a wide range of $k_{\text{cat}}/K_{\text{m}}$ values. The data in Figure 4 show that all three effector-bound states process an alternative substrate with a ' k ' value within ~10-fold of that of the cognate substrate. Multiple NDPs can serve as substrates for hRR and ScRR regardless of which effector is bound, although there can be a >1000-fold difference in the highest and lowest $k_{\text{cat}}/K_{\text{m}}$ values.^{17,24,28,39,40} For example, we find that for ATP-bound hRR, CDP is the favored substrate as expected; however, the $k_{\text{cat}}/K_{\text{m}}$ values for ADP, GDP, and UDP are within 100-fold of the value for CDP. The yeast enzyme is similar but has a 100-fold lower $k_{\text{cat}}/K_{\text{m}}$ for GDP than for ADP and UDP. In the dGTP-bound state, the optimal ADP substrate is favored over CDP by only ~10-fold, while there is 100-fold discrimination against UDP relative to ADP. The $k_{\text{cat}}/K_{\text{m}}$ for GDP is at least 1000-fold lower than the value for ADP, although an accurate measurement was not possible because of a low level of hydrolysis of the dGTP effector to form dGDP. Analysis of the dTTP-bound state of RR demonstrates >10-fold discrimination against CDP relative to the optimal substrate GDP. For hRR bound to dTTP, both ADP and UDP have $k_{\text{cat}}/K_{\text{m}}$ values that are 100-fold lower than that of the optimal substrate, GDP. However, the dTTP-bound state of ScRR displays further discrimination over UDP, which was not detectable in our assay.

Several groups previously used internal competition or individual substrate assays to quantify specificity for RR enzymes from diverse species. In some studies, the data were interpreted quantitatively in terms of relative specificity constants, while others report the relative activities when substrates are present at equimolar concentrations.^{17,24,28,39,40} These inquiries provide important context and calibration points for these new data, and they are summarized in Figure

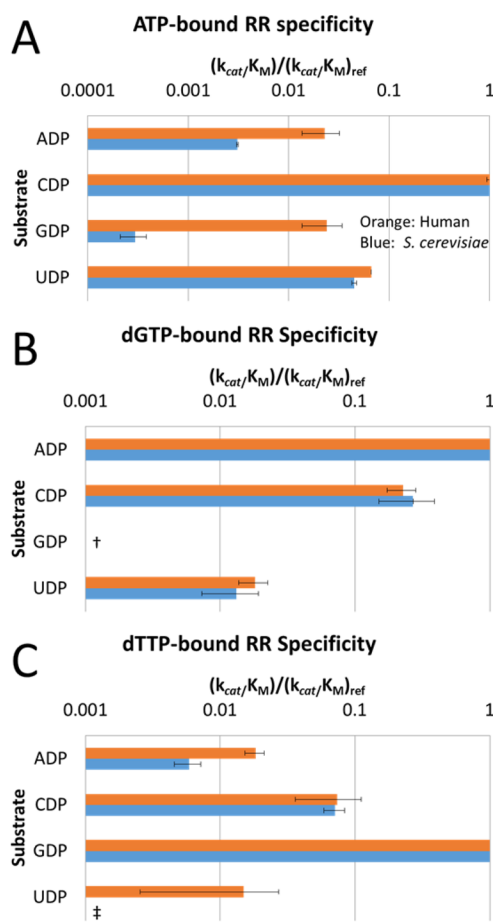


Figure 4. Measurement of native hRR and ScRR specificities. Data are shown as dimensionless k values. k values may be considered equal to the proportion of each product formed relative to the reference product when the two substrates are present at equimolar concentrations. (A) Specificity of hRR (orange bars) and ScRR (blue bars) in the presence of 1 mM ATP. (B) Like panel A, but in the presence of 1 mM ATP and 0.75 mM dGTP. (C) Like panel A, but in the presence of 1 mM ATP and 1.6 mM dTTP. ‡ indicates a product that was not present in sufficient quantity to accurately measure its formation. † indicates a product that co-elutes with a hydrolysis product from an effector. The specific activity for ScRR across all substrates in the presence of 1 mM ATP was $0.11 \pm 0.017 \text{ mol s}^{-1} (\text{mol of ScRR})^{-1}$.²⁰ See Figures 5 and 7 for hRR specific activity values.²⁰ Similar values were obtained when ATP was present in the presence or absence of dGTP or dTTP.

S1. When compared across RR enzymes from different species and methods of analysis, the data confirm the universal core selection rules but also reveal some variation in the relative rates for nonoptimal substrates. For example, the data presented here show good qualitative agreement with the allosteric rules derived from studies of EcRR, though ATP-bound EcRR processes UDP more efficiently and dGTP-bound EcRR processes CDP less efficiently than hRR or ScRR.¹⁷

As described above, current models of eukaryotic and bacterial RRs include key interactions between effector nucleobases and amino acids proximal to D287 and the conserved Q288 (hRR numbering) in loop 2. However, functional tests of the proposed chemical interactions between loop 2 and nucleotide effectors remain comparatively limited, especially for the biomedically important hRR. Therefore, we systematically varied effector nucleobase functional groups and

quantitatively compared the resulting effects on hRR substrate specificity.

Identification of the Chemical Groups Responsible for Allosteric Regulation of hRR Specificity by dTTP. To determine the molecular features of dTTP that contribute to substrate discrimination, we tested the specificities directed by a set of pyrimidine nucleotide effector analogues (2-thio-dTTP, 5FdUTP, dCTP, 5-methyl-dCTP, dUTP, and dZeb) (Figure 5). When assayed individually at 100 μM , all of the analogues tested except dCTP and 5-methyl-dCTP result in significant RR activity that is within 3–5-fold of that observed in the presence of dTTP. The concentration of 100 μM is ~ 200 -fold greater than the measured K_D for dTTP binding. For comparison, this concentration is also 2-fold higher than the concentration of dTTP in control reaction mixtures. The ability to induce activity similar to that of the native effector is consistent with functional binding of the analogues to the S-site. Nonetheless, it is possible that the S-site may not be fully saturated even though this concentration is significantly greater than the dissociation constant for dTTP (see Figure 8B). However, for most of the analogues, the total rate of product accumulation is within a few-fold of that of the control reaction of the mixture containing 50 μM dTTP.

Amounts of products formed are sufficient to accurately identify the optimal substrate and observe reproducible effects on specificity, except when dCTP or 5-methyl-dCTP is used as an effector. Consistent with previous biochemical studies of RR, hRR discriminates exquisitely against the N4 group of dCTP.^{41,42} This observation is also consistent with a crystal structure of hRR in complex with dTTP and GDP, which features O4 of dTTP proximal to the backbone amide groups of D287, Q288, and G289 (PDB entry 3HND) (Figure 6).²⁰ Removal of the 5-methyl group from dTTP reduces the level of discrimination between GDP and CDP by ~ 2 -fold (compare dTTP and dUTP). This functional group packs against a side chain methylene group in the S-site of the hRR structure model, and replacement with a fluorine atom increases the k for GDP, consistent with a nonpolar contact (compare dUTP and 5FdUTP) (Figure 5). Substitution of O2 with a sulfur atom also increases specificity for GDP, indicating that the larger size and reduced electronegativity can be accommodated by the S-site at this position.

Importantly, removal of the O4 atom and the concomitant deprotonation of the N3 atom in dZeb are sufficient to eliminate discrimination between GDP and CDP (compare dUTP and dZeb). This result is consistent with interactions involving these functional groups contributing to specificity for GDP over CDP; however, the overall shape of the residual pyrimidine base still enforces some degree of native specificity. The structural model of the hRR–dTTP–GDP complex predicts interactions between O4 and N3 of dTTP and the backbone of loop 2 and nearby N270, while the O2 group does not appear to be involved in a contact (PDB entry 3HND) (Figure 6A). Thus, the results reveal a pattern of sensitivity to chemical modification consistent with interactions involving primarily N3 and O4 with hydrophobic packing interactions with the 5-methyl group contributing incrementally to discrimination between CDP and GDP.

N1 of the Purine Nucleobase Is a Primary Determinant That Differentiates Allosteric Regulation by dGTP versus ATP. Structures of eukaryotic RR in which dGTP/ADP and AMPPNP/CDP are the effector/substrate ligands bound to the S-site and C-site suggest differential interactions with the

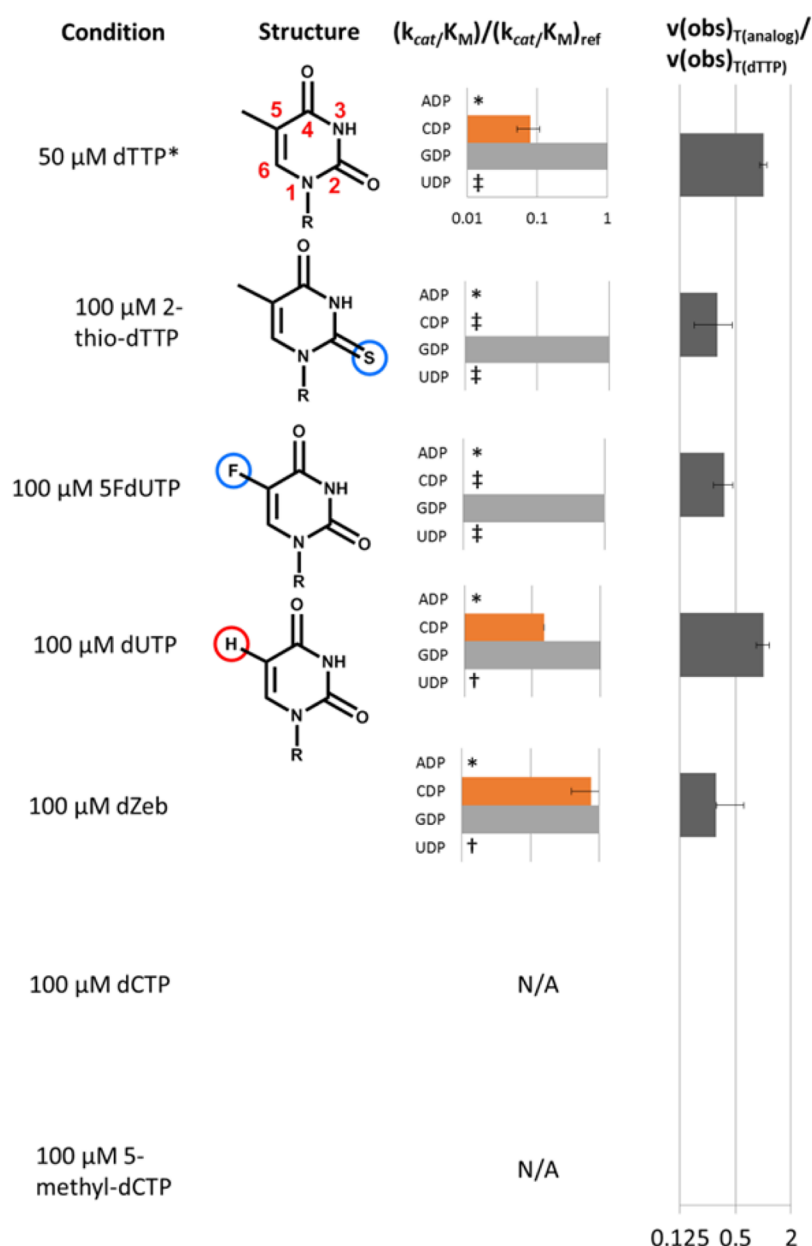


Figure 5. Specificities directed by a series of pyrimidine effector analogues. “R” denotes the deoxyribose triphosphate moiety. Functional groups on the nucleobase of dTTP are numbered. Altered functional groups are highlighted. Red denotes a functional group that has been replaced with a hydrogen atom. Blue denotes a hydrogen atom that has been replaced with a functional group. Specificity is defined as in Figure 4. ‡ indicates a product that was not present in sufficient quantity to accurately measure its formation. † indicates a product that co-elutes with a hydrolysis product from an effector. ADP was not included (*). Velocity ratios represent the total observed reaction velocity for the indicated analogue relative to the total velocity for dTTP. The specific activity across all substrates in the presence of 50 μ M dTTP was $0.0066 \pm 0.00052 \text{ mol s}^{-1} (\text{mol of hRRM1})^{-1}$.²⁰

purine nucleobase at the S-site (PDB entries 2CVX and 2CVU in panels B and C, respectively, of Figure 6). We identified the chemical features of the purine effectors ATP and dGTP that drive specificity for CDP and ADP, respectively, by testing a series of purine effector analogues (2-aminopurine-drTP, N2dATP, 7-deaza-dATP, 7-deaza-dGTP, and dTTP) for their ability to allosterically regulate hRR.

Because both the S-site and the A-site bind dATP, we first considered whether confounding effects due to A-site binding could lead to inaccuracies in observed specificity. Importantly, we observed that all effectors tested stimulated RR activity to some degree at concentrations that are fully inhibitory for dATP.¹⁵ This observation suggests that the analogues do not

inhibit hRR to the same extent as dATP. Moreover, the presence or absence of A-site ligands is not known to have significant effects on substrate specificity (compare Figure 4 with Figures 5 and 7). Also noteworthy is the fact that none of the dATP analogues abrogated substrate processing. It is therefore possible that they were unable to bind in the A-site. Such binding would likely lead to inhibition because the analogues all lack a 2'-hydroxyl group and dATP A-site binding inhibits eukaryotic class I RR.¹⁴ Thus, the observed specificity in the presence of nucleotide analogues is most likely due to S-site binding. This assumption is tested directly for dTTP and 2-aminopurine-drTP (Figure 8). Nonetheless, modulation of overall activity by A-site binding cannot be entirely excluded

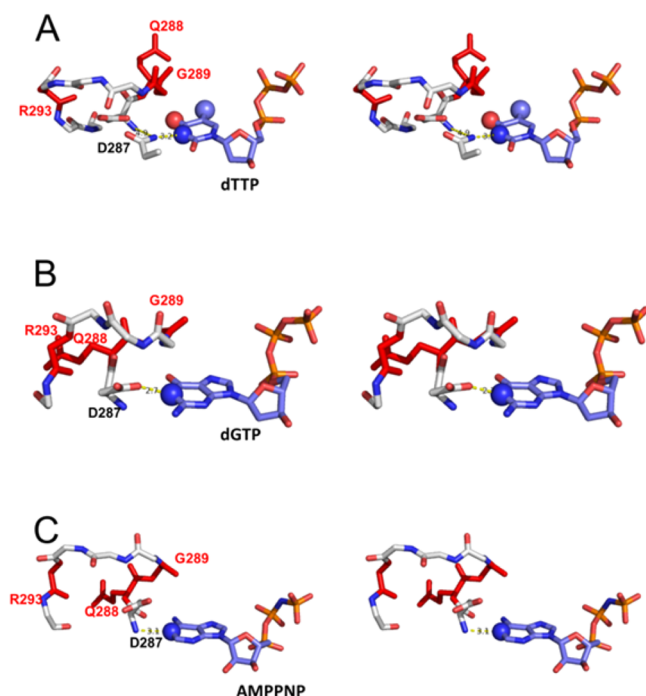


Figure 6. Structures of eukaryotic RR bound to S-site ligands. (A) Crystal structure of hRR bound to dTTP and GDP (not shown) (PDB entry 3HND, 3.21 Å resolution).²⁰ (B) Crystal structure of ScRR bound to dGTP and ADP (not shown) (PDB entry 2CVX, 2.2 Å resolution). (C) Crystal structure of ScRR bound to AMPPNP and CDP (not shown) (PDB entry 2CVU, 2.9 Å resolution).⁷ S-Site ligands are shown as dark blue sticks. Atoms that perturb specificity when modified are shown as small spheres. Loop 2 amino acids are shown as white sticks. Q288, G289, and R293 are shown as red sticks. Potential contacts involving D287 are shown as yellow dashes.

even though there is no current evidence that nucleotide binding at the A-site influences substrate specificity at the C-site.

As shown in Figure 7, the specificities observed with purine analogues strongly suggest that the protonation state of the N1 atom on the purine ring and the presence of a guanosine O6 group determine whether hRR recognizes it as ATP or dGTP. Most purine nucleobase modifications have relatively weak effects on the total activity [$v_{(\text{obs})\text{T}(\text{analogue})}/v_{(\text{obs})\text{T}(\text{dGTP})}$] at the concentration of effector tested (100 μM). The purine N7 atom is dispensable for specificity determination because 7-deaza-dATP and 7-deaza-dGTP have specificity comparable to that of ATP and dGTP, respectively. Furthermore, N2dATP and 2-aminopurine-drTP both direct C-site specificity for CDP, while dITP directs specificity for ADP. This result argues strongly against any model in which either guanosine N2 or adenosine N6 is the main determinant of specificity. These positions are proximal to the loop 2 peptide backbone, but they do not appear to influence C-site specificity (PDB entries 2CVX and 2CVU in panels B and C, respectively, of Figure 6). The experimental results strongly implicate the N1 atom of the purine nucleobase in making a large binary contribution to determining whether the enzyme has an optimal $k_{\text{cat}}/K_{\text{m}}$ for ADP or CDP. The identity of the group at position 6 is also likely to contribute to the specificity directed by dGTP; however, removal of the O6 group necessarily results in deprotonation of the N1 group, making these variables difficult to deconvolute.

Evidence That dITP and 2-Aminopurine-drTP Direct Specificity by Binding at the Specificity Site.

When dNTP analogues are added to *in vitro* hRR specificity assays as the only effector, they stimulate NDP reduction and cause shifts in specificity, consistent with S-site binding. However, mammalian RR has three known nucleotide binding sites, and *Pseudomonas aeruginosa* RR is known to bind two ATP molecules in its N-terminal ATP cone domain.^{14,15,43} Given the complexity of RR regulation and nucleotide binding, we tested whether nucleotide analogue triphosphates and native dNTP effectors compete for S-site binding. The possibility of alternative binding at the A-site is strongest for the purine analogues because they are chemically most similar to dATP, a ligand that is known to bind to both the S-site and the A-site of hRR. However, the native effector dTTP is known to bind at only the S-site, and the specificity it directs is different from the specificity directed by any purine effector or effector analogue.^{20,23} Therefore, competition between dTTP binding and analogue binding at the S-site should necessarily result in both a concentration-dependent change in the proportions of the products formed and a weaker apparent affinity for dTTP.

As described above, data gathered in the presence of dITP and 2-aminopurine-drTP as effectors support the interpretation that the N1 atom directs specificity for purines. Accordingly, we tested whether dITP competes with dITP or 2-aminopurine-drTP for binding at the S-site (Figure 8). When a mixture of hRR and 50 μM dITP or 2-aminopurine-drTP is challenged with dTTP, the specificity directed by the analogue is suppressed in a concentration-dependent manner (Figure 8A). The specificity of hRR for GDP over CDP can be used to estimate the degree to which the S-site is occupied by dITP. The data fit to hyperbolic binding isotherms (Figure 8B,C) that in the presence of dITP or 2-aminopurine-drTP yield apparent dissociation constants for dITP that are approximately 2 orders of magnitude higher than the observed value of 0.46 μM . Assuming a simple competitive binding model, the dissociation constants for dITP and 2-aminopurine-drTP are in the range of 100–200 nM. These values are comparable to the dissociation constant for binding of dGTP to murine RR (700 nM).²³ While binding of some of the tested analogues at additional sites on hRR cannot be entirely excluded, the results are most consistent with a model in which dITP and 2-aminopurine-drTP exert their effects on specificity through S-site binding.

The Side Chain of D287 in Loop 2 of hRR Is Essential for Specificity Regulation by dGTP and dITP, but Not ATP.

Although a unifying model of RR allostery has yet to be fully realized, the available ScRR structures with effectors bound in the S-site provide a context for identifying potential interactions that may interpret the signals directed by the N1 and O6 groups of purine effectors (Figure 6). In the structure of ScRR containing AMPPNP in the S-site, the N1 atom of the adenine nucleobase accepts a hydrogen bond from the backbone amide group of D287 in loop 2 while the side chain is pointed away from the S-site (PDB entry 2CVU).^{44,45} In contrast, the protonated N1 group of dGTP acts as a hydrogen bond donor and contacts the carboxylic acid moiety of D287 in the dGTP/ADP structure of ScRR (PDB entry 2CVX). In a crystal structure of hRR with dITP bound in the S-site, the nucleobase does not contact D287. Instead, D287 forms a hydrogen bond with N270, which in turn contacts the N3 group of dITP (Figure 6, PDB entry 3HND).^{44,46,47} These different interactions with D287 appear to favor alternative conformations of loop 2. Consistent with this notion, previous

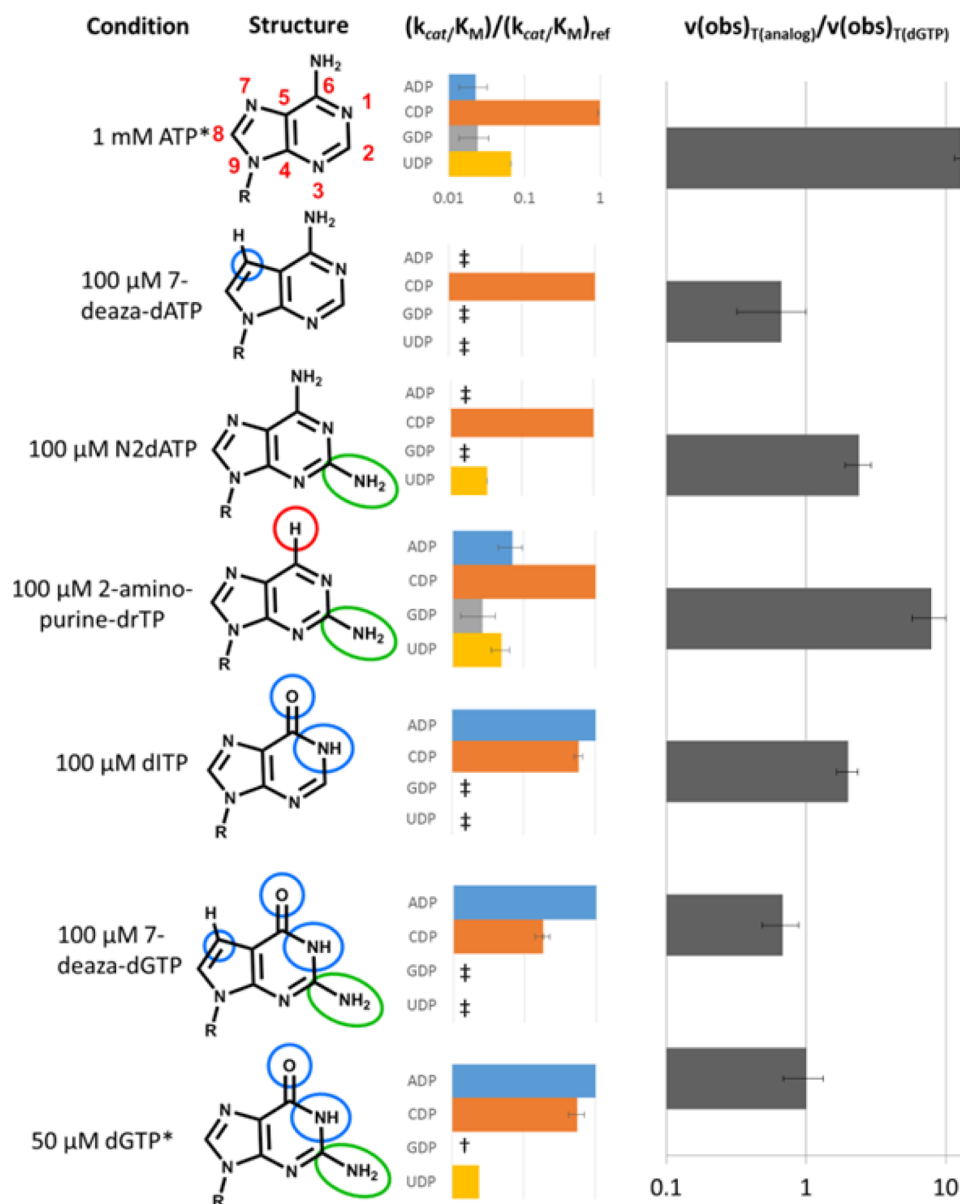


Figure 7. Specificities directed by a series of purine effector analogues. R denotes the deoxyribose triphosphate moiety, except that ATP has a ribose triphosphate moiety. Functional groups on the nucleobase of ATP are numbered. Altered functional groups are highlighted. Red denotes a functional group that has been replaced with a hydrogen atom. Blue denotes a functional group that has been replaced. Green denotes a hydrogen atom that has been replaced with a functional group. Specificity is defined as in Figure 4. ‡ indicates a product that was not present in sufficient quantity to accurately measure its formation. † indicates a product that co-elutes with a hydrolysis product from an effector. Velocity ratios represent the total observed reaction velocity for the indicated analogue relative to the total velocity for dGTP. The specific activity across all substrates in the presence of 50 μ M dGTP was $0.0055 \pm 0.0017 \text{ mol s}^{-1} (\text{mol of hRRM1})^{-1}$.²⁰

studies of RR function *in vivo* showed that a D287A mutation in ScRR results in larger cellular dCTP and dTTP pools.⁴⁸ Together, the structure modeling and available mutagenesis data suggest that the D287 side chain may play a role in the recognition of dGTP and dTTP but is not apparently involved in contacting ATP (Figure 6).

To address the potential role of D287 in hRR function, we constructed the D287A mutant of hRR and assayed its specificity in the presence of the native effectors ATP, dGTP, and dTTP (Figure 9). This mutant shows essentially identical specificity when ATP is used as the effector. In contrast, this mutant fails to efficiently discriminate among any specificity drivers intrinsic to either dGTP or dTTP and favors CDP as the optimal substrate for all three effectors. When dGTP is used

as the effector, the D287A mutant has the highest k_{cat}/K_M for CDP while wild-type hRR prefers ADP. When dTTP is used as the effector, only GDP and CDP are processed detectably, which is somewhat similar to the case for the native enzyme. However, the k_{cat}/K_M of CDP is greater than that of GDP by 10-fold. Thus, the primary effect of deleting the D287 side chain is to silence allosteric information provided by the dGTP and dTTP nucleobase functional groups and shift hRR substrate selection toward ATP-driven specificity.

DISCUSSION

In summary, the results provide a chemically detailed picture of the effector functional groups responsible for directing the allosteric regulation of hRR substrate specificity. The data

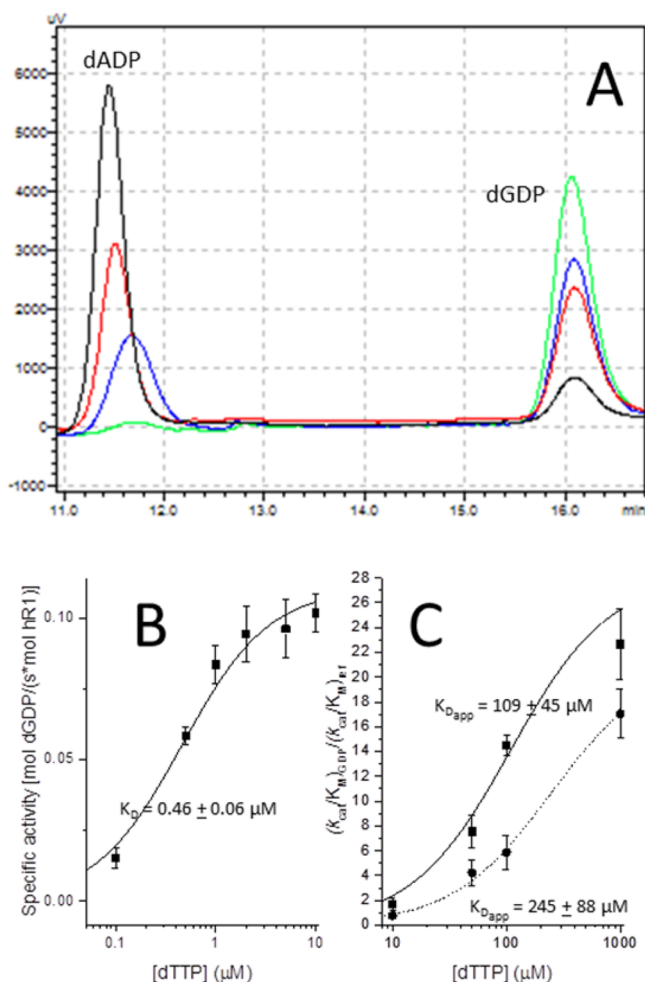


Figure 8. Competition between purine effector analogues and the natural S-site effector dTTP. dTTP or 2-aminopurine-drTP (50 μM) was challenged with dTTP in the presence of all four NDP substrates. Substrates were present at a concentration of 600 μM . (A) Representative chromatograms from a competition assay. hRR in the presence of 50 μM dTTP was challenged with 10 μM dTTP (black), 50 μM dTTP (red), 100 μM dTTP (blue), or 1000 μM dTTP (green). The specificity directed by dTTP (dADP favored) is suppressed by specificity directed by dTTP (dGDP favored). (B) Measurement of the dissociation constant between hRRM1 and dTTP. GDP reductase activity in the presence of 1.2 mM GDP was measured in the presence of 0 μM dTTP, 0.1 μM dTTP, 0.5 μM dTTP, 1 μM dTTP, 2 μM dTTP, 5 μM dTTP, and 10 μM dTTP. (C) Plot of [dTTP] vs the relative second-order rate constant for GDP over CDP in the presence of 50 μM dTTP (●, dashed line) or 50 μM 2-aminopurine-drTP (■, solid line). In panels B and C, data can be fit to a hyperbolic binding isotherm to derive an apparent dissociation constant for dTTP.

provide experimental evidence that N1 of the purine nucleobase is a primary chemical signal that differentiates specificity directed by the effector dGTP versus ATP/dATP. Guanosine O6 is also likely to contribute to specificity, as suggested by structural models of both eukaryotic RR and EcRR. However, effects of individual functional group modifications at this position also affect the conjugation of N1, complicating interpretation of the effects on specificity. Although adenosine N6 figures prominently in structural models, this functional group does not appear play a major role in allosteric communication. This interpretation is based primarily on the observation that 2-aminopurine-drTP directs

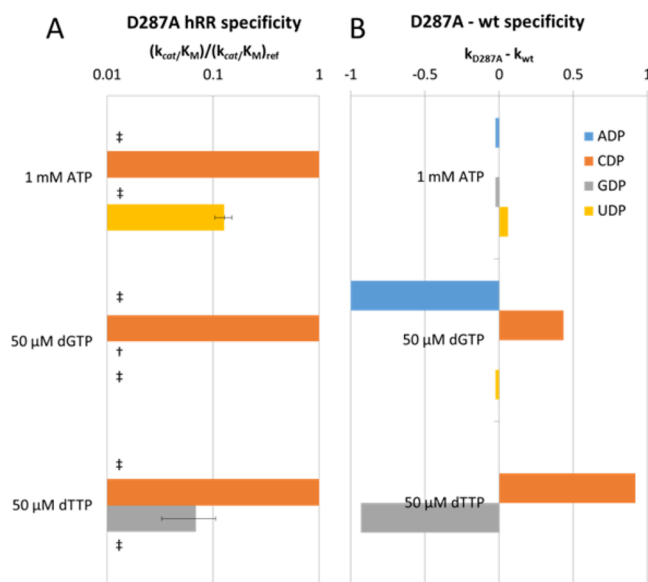


Figure 9. Effects of the D287A substitution on hRR substrate recognition. (A) Specificity of D287A hRR under the indicated conditions. Specificity is defined as in Figure 4. ‡ indicates a product that was not present in sufficient quantity to accurately measure its formation. † indicates a product that co-elutes with a hydrolysis product from an effector. The specific activity for D287A hRR in the presence of 1 mM ATP was $0.053 \pm 0.002 \text{ mol s}^{-1} (\text{mol of hRRM1})^{-1}$, in the presence of 50 μM dGTP $0.0028 \pm 0.00048 \text{ mol s}^{-1} (\text{mol of hRRM1})^{-1}$, and in the presence of 50 μM dTTP $0.0072 \pm 0.0025 \text{ mol s}^{-1} (\text{mol of hRRM1})^{-1}$. (B) For each substrate, the difference between its $^{\dagger}k$ in the presence and absence of the D287A mutation is shown. Negative values indicate that the D287A mutant prefers the substrate less than the wild type does; positive values indicate that the opposite is true. For example, if a substrate is not appreciably processed by wild-type hRR but is the favored substrate for D287A hRR, the difference has a value of 1.

CDP specificity like ATP despite the fact that it has an exocyclic N2 atom like dGTP and lacks an N6 atom like that characteristic of adenosine.

The data suggest that the exocyclic amine of dCTP acts as an antideterminant for overall effector function. This interpretation is based on the ability of dZeb to act as an effector. The dZeb nucleobase is essentially identical to cytosine but lacks an exocyclic amine at position 4 on the pyrimidine ring. Nonetheless, at equivalent concentrations (100 μM), dZeb is able to direct hRR catalytic activity while dCTP fails to do so. Importantly, dZeb has greatly reduced specificity for GDP over CDP when compared to the specificity directed by the native dTTP effector. This effect may be due to the deprotonated N3 atom of the zebularine nucleobase, which could function like the deprotonated N1 atom of adenosine and form interactions that drive specificity for CDP. Surprisingly, dZeb drives GDP reduction in spite of its lack of a 5-methyl group, an O4 group, and a deprotonated N3 atom relative to the native dTTP effector. Thus, none of these characteristic functional groups is absolutely required to favor the loop 2 conformation that is specific for GDP. Interestingly, none of the pyrimidine modifications caused hRR to adopt a new preferred substrate other than GDP. Together, the results reveal an S-site that is highly sensitive to the presence of an N4 amine, but otherwise remarkably accommodating of variation in the size and electronic properties of the pyrimidine nucleobase.

The observation that D287A mutant hRR primarily reduces CDP in the presence of any of the three effectors is consistent with the presence of functional interactions between dGTP/dTTP and the side chain of D287. In current structural models of eukaryotic RR, the adenosine N1 atom contacts the backbone amide of D287, while the protonated N1 atom of dGTP can hydrogen bond to the carboxylic acid side chain (PDB entries 2CVU and 2CVX). Loss of this interaction could weaken the ability of dGTP to induce the loop 2 conformation that is optimal for ADP binding. While the D287 side chain does not directly contact dTTP, it is part of a network of hydrogen bonding interactions that includes N270 (PDB entry 3HND). Disruption of this network could weaken the ability of dTTP to induce loop 2 conformations that favor interactions with GDP in the C-site.

As illustrated in Figure 2A, the conservation of loop 2 sequence is very strong and mutations at these positions can generate aberrant substrate recognition phenotypes in ScRR,^{45,48,49} consistent with its central role in allosteric communication. The major features of substrate recognition are conserved among RRs from various species, and the roles of conserved amino acids in loop 2 are likely to be analogous (Figure S1). It is less clear how phylogenetic variation in loop 2 affects structure–function relationships involved in allostery. Comparisons of structural models and inferences from functional experiments are consistent with a role for R293 in interacting with the phosphate groups and nucleobase of the substrate.⁴⁵ However, structures of ScRR do not show direct contacts between R293 and the phosphate groups of the substrate, raising a potential issue with interpretation of these structural models.⁷ Q288 occupies a similar position in the EcRR and ScRR structural models of the dATP/AMPPNP-bound states (Figure 2), consistent with a conserved role in stabilizing the loop 2 structure. The corresponding positions of Q288 differ more significantly between the bacterial and eukaryotic RR models with dGTP or dTTP bound in the S-site (Figure S2). Phylogenetic comparative sequence analyses show that the identity of D287 is not conserved among all species, though it is strongly conserved among eukaryotes. While the D287 side chain of ScRR contacts N1 of dGTP, a similar interaction is not observed for the corresponding serine residue in EcRR (PDB entries 2CVX and 5CNU). N1 is instead contacted by the conserved Q294 (EcRR numbering), and it is possible that this contact is key for EcRR effector recognition. Additional structure–function studies of RR loop 2 interactions and conformations are required to test proposed functional interactions. Importantly, although structural models are vital tools for model building and hypothesis generation, the biochemical data presented here represent a complementary yet independent line of inquiry that is foundational for any model of hRR allostery.

The ability to quantify specificity for all four NDP substrates in the presence of a range of nucleotide analogues reveals several important general features of RR substrate discrimination. A well-known characteristic of RRs that is further documented here is the ability of the enzyme to accept multiple alternative substrates even in the presence of a single dNTP effector. Interestingly, CDP has the highest $k_{\text{cat}}/K_{\text{M}}$, or its value is within ~10-fold of that of the optimal NDP substrate for both hRR and ScRR regardless of which effector is bound. Additionally, the D287A hRR mutant is defective in allosteric communication induced by dGTP and dTTP and reduces primarily CDP regardless of the identity of the effector

nucleobase. These results together suggest that the CDP-reducing conformation of loop 2 may be a default state with respect to specificity. It has previously been suggested that loop 2 conformations exist in dynamic equilibrium and key interactions with the effector nucleobase serve to perturb that equilibrium. In this model, binding of dGTP or dTTP acts to shift the conformation or conformational ensemble away from this default state.¹²

Indeed, interactions between protein and ligand are typically accompanied by a redistribution of thermally accessible conformations.^{50,51} Mutations can cause multiple direct and indirect changes in allosteric communication,^{52,53} and pinning down the individual roles of particular interactions is difficult. Importantly, Cooperman and colleagues have developed foundational equilibrium thermodynamic schemes that describe levels of activity based on the population of effector- and substrate-bound states.^{15,16,54} Current challenges now include the need to incorporate specific structural and functional detail and to account for the contributions from both optimal and nonoptimal substrates for a given effector. Moreover, a complete comprehension of RR allostery necessarily requires understanding the linkages among effector and substrate binding thermodynamics, the dynamic behavior of loop 2 conformations, and other elements of RR protein structure.

■ ASSOCIATED CONTENT

📄 Supporting Information

The Supporting Information is available free of charge on the ACS Publications website at DOI: 10.1021/acs.biochem.6b00594.

Summary of RR specificity measurements from the literature (Figure S1) and comparison of loop 2 conformations among EcRR, ScRR, and hRR (Figure S2) (PDF)

■ AUTHOR INFORMATION

Corresponding Author

*E-mail: meh2@case.edu. Phone: 216-368-4779.

Funding

This research was supported by Grant GM100887 to C.G.D. and Grant GM096000 to M.E.H. A.J.K. was supported by National Institute of General Medical Sciences Predoctoral Training Grant T32 GM008056.

Notes

The authors declare no competing financial interest.

■ ABBREVIATIONS

RR, ribonucleotide reductase; hRR, human ribonucleotide reductase; ScRR, *S. cerevisiae* ribonucleotide reductase; TmRR, *T. maritima* ribonucleotide reductase; EcRR, *E. coli* ribonucleotide reductase; NDP, nucleoside diphosphate; dNDP, deoxyribonucleoside diphosphate; dNTP, deoxyribonucleoside triphosphate; A-site, Activity site; S-site, Specificity site; C-site, Catalytic site; v_{obs} , observed velocity; $^{\circ}k$, relative second-order rate constant $k_{\text{cat}}/K_{\text{M}}$ for an NDP substrate relative to a given reference substrate $[(k_{\text{cat}}/K_{\text{M}})_{\text{NDP}}/(k_{\text{cat}}/K_{\text{M}})_{\text{reference}}]$; 5FdUTP, 5-fluorodeoxyuridine triphosphate; dUTP, deoxyuridine triphosphate; dZeb, deoxyzebularine triphosphate; 2-aminopurine-drTP, 2-aminopurine-deoxyribose triphosphate; N2dATP, 2-amino-deoxyadenosine triphosphate; dITP, deoxyinosine triphosphate; PDB, Protein Data Bank.

■ REFERENCES

- (1) Changeux, J.-P. (2012) Allostery and the Monod-Wyman-Changeux model after 50 years. *Annu. Rev. Biophys.* 41, 103–133.
- (2) Wegner, A., Meiser, J., Weindl, D., and Hiller, K. (2015) How metabolites modulate metabolic flux. *Curr. Opin. Biotechnol.* 34, 16–22.
- (3) Benesch, R., and Benesch, R. E. (1963) Some relations between structure and function in hemoglobin. *J. Mol. Biol.* 6, 498–505.
- (4) Gerhart, J. C., and Schachman, H. K. (1968) Allosteric interactions in aspartate transcarbamylase. II. Evidence for different conformational states of the protein in the presence and absence of specific ligands. *Biochemistry* 7, 538–552.
- (5) Srinivasan, B., Forouhar, F., Shukla, A., Sampangi, C., Kulkarni, S., Abashidze, M., Seetharaman, J., Lew, S., Mao, L., Acton, T. B., Xiao, R., Everett, J. K., Montelione, G. T., Tong, L., and Balaram, H. (2014) Allosteric regulation and substrate activation in cytosolic nucleotidase II from *Legionella pneumophila*. *FEBS J.* 281, 1613–1628.
- (6) Brown, N. C., and Reichard, P. (1969) Role of effector binding in allosteric control of ribonucleoside diphosphate reductase. *J. Mol. Biol.* 46, 39–55.
- (7) Xu, H., Faber, C., Uchiki, T., Fairman, J. W., Racca, J., and Dealwis, C. (2006) Structures of eukaryotic ribonucleotide reductase I provide insights into dNTP regulation. *Proc. Natl. Acad. Sci. U. S. A.* 103, 4022–4027.
- (8) Huang, M., Zhou, Z., and Elledge, S. J. (1998) The DNA replication and damage checkpoint pathways induce transcription by inhibition of the Crt1 repressor. *Cell* 94, 595–605.
- (9) Zhang, Z., An, X., Yang, K., Perlstein, D. L., Hicks, L., Kelleher, N., Stubbe, J., and Huang, M. (2006) Nuclear localization of the *Saccharomyces cerevisiae* ribonucleotide reductase small subunit requires a karyopherin and a WD40 repeat protein. *Proc. Natl. Acad. Sci. U. S. A.* 103, 1422–1427.
- (10) Zimanyi, C. M., Chen, P. Y.-T., Kang, G., Funk, M. A., and Drennan, C. L. (2016) Molecular basis for allosteric specificity regulation in class Ia ribonucleotide reductase from *Escherichia coli*. *eLife* 5, e07141.
- (11) Yao, R., Zhang, Z., An, X., Bucci, B., Perlstein, D. L., Stubbe, J., and Huang, M. (2003) Subcellular localization of yeast ribonucleotide reductase regulated by the DNA replication and damage checkpoint pathways. *Proc. Natl. Acad. Sci. U. S. A.* 100, 6628–6633.
- (12) Larsson, K.-M., Jordan, A., Eliasson, R., Reichard, P., Logan, D. T., and Nordlund, P. (2004) Structural mechanism of allosteric substrate specificity regulation in a ribonucleotide reductase. *Nat. Struct. Mol. Biol.* 11, 1142–1149.
- (13) Thelander, L., and Reichard, P. (1979) Reduction of ribonucleotides. *Annu. Rev. Biochem.* 48, 133–158.
- (14) Ando, N., Li, H., Brignole, E. J., Thompson, S., McLaughlin, M. L., Page, J. E., Asturias, F. J., Stubbe, J., and Drennan, C. L. (2016) Allosteric inhibition of human ribonucleotide reductase by dATP entails the stabilization of a hexamer. *Biochemistry* 55 (2), 373–381.
- (15) Kashlan, O. B., Scott, C. P., Lear, J. D., and Cooperman, B. S. (2002) A comprehensive model for the allosteric regulation of mammalian ribonucleotide reductase. Functional consequences of ATP- and dATP-induced oligomerization of the large subunit. *Biochemistry* 41, 462–474.
- (16) Cooperman, B. S., and Kashlan, O. B. (2003) A comprehensive model for the allosteric regulation of Class Ia ribonucleotide reductases. *Adv. Enzyme Regul.* 43, 167–182.
- (17) Rofougaran, R., Crona, M., Vodnala, M., Sjöberg, B.-M., and Hofer, A. (2008) Oligomerization status directs overall activity regulation of the *Escherichia coli* class Ia ribonucleotide reductase. *J. Biol. Chem.* 283, 35310–35318.
- (18) Rofougaran, R., Vodnala, M., and Hofer, A. (2006) Enzymatically active mammalian ribonucleotide reductase exists primarily as an $\alpha\beta_2$ octamer. *J. Biol. Chem.* 281, 27705–27711.
- (19) Wang, J., Lohman, G. J., and Stubbe, J. (2007) Enhanced subunit interactions with gemcitabine-5'-diphosphate inhibit ribonucleotide reductases. *Proc. Natl. Acad. Sci. U. S. A.* 104, 14324–14329.
- (20) Fairman, J. W., Wijerathna, S. R., Ahmad, M. F., Xu, H., Nakano, R., Jha, S., Prendergast, J., Welin, R. M., Flodin, S., Roos, A., Nordlund, P., Li, Z., Walz, T., and Dealwis, C. G. (2011) Structural basis for allosteric regulation of human ribonucleotide reductase by nucleotide-induced oligomerization. *Nat. Struct. Mol. Biol.* 18, 316–322.
- (21) Reichard, P. (2002) Ribonucleotide reductases: the evolution of allosteric regulation. *Arch. Biochem. Biophys.* 397, 149–155.
- (22) Eriksson, M., Uhlin, U., Ramaswamy, S., Ekberg, M., Regnström, K., Sjöberg, B.-M., and Eklund, H. (1997) Binding of allosteric effectors to ribonucleotide reductase protein R1: reduction of active-site cysteines promotes substrate binding. *Structure* 5, 1077–1092.
- (23) Scott, C. P., Kashlan, O. B., Lear, J. D., and Cooperman, B. S. (2001) A quantitative model for allosteric control of purine reduction by murine ribonucleotide reductase. *Biochemistry* 40, 1651–1661.
- (24) Hendricks, S. P., and Mathews, C. K. (1997) Regulation of T4 Phage Aerobic Ribonucleotide Reductase SIMULTANEOUS ASSAY OF THE FOUR ACTIVITIES. *J. Biol. Chem.* 272, 2861–2865.
- (25) Sievers, F., Wilm, A., Dineen, D., Gibson, T. J., Karplus, K., Li, W., Lopez, R., McWilliam, H., Remmert, M., Söding, J., Thompson, J. D., and Higgins, D. G. (2011) Fast, scalable generation of high-quality protein multiple sequence alignments using Clustal Omega. *Mol. Syst. Biol.* 7, 539.
- (26) Goujon, M., McWilliam, H., Li, W., Valentin, F., Squizzato, S., Paern, J., and Lopez, R. (2010) A new bioinformatics analysis tools framework at EMBL–EBI. *Nucleic Acids Res.* 38, W695–W699.
- (27) Benson, D. A., Clark, K., Karsch-Mizrachi, L., Lipman, D. J., Ostell, J., and Sayers, E. W. (2015) GenBank. *Nucleic Acids Res.* 43, D30.
- (28) Hofer, A., Ekanem, J. T., and Thelander, L. (1998) Allosteric regulation of *Trypanosoma brucei* ribonucleotide reductase studied in vitro and in vivo. *J. Biol. Chem.* 273, 34098–34104.
- (29) Cha, S. (1968) Kinetics of enzyme reactions with competing alternative substrates. *Mol. Pharmacol.* 4, 621–629.
- (30) Schellenberger, V., Siegel, R. A., and Rutter, W. J. (1993) Analysis of enzyme specificity by multiple substrate kinetics. *Biochemistry* 32, 4344–4348.
- (31) Cleland, W. W. (2005) The use of isotope effects to determine enzyme mechanisms. *Arch. Biochem. Biophys.* 433, 2–12.
- (32) Melander, L., and Saunders, W. H. (1980) *Reaction Rates of Isotopic Molecules*, Wiley, New York.
- (33) Kohen, A., and Limbach, H. H. (2005) *Isotope Effects In Chemistry and Biology*, Taylor & Francis, New York.
- (34) Anderson, V. E. (2015) Multiple alternative substrate kinetics. *Biochim. Biophys. Acta, Proteins Proteomics* 1854 (11), 1729–1736.
- (35) Cha, S. (1968) Kinetics of enzyme reactions with competing alternative substrates. *Mol. Pharmacol.* 4, 621–629.
- (36) Northrop, D. B. (1983) Fitting enzyme-kinetic data to VK. *Anal. Biochem.* 132, 457–461.
- (37) Northrop, D. B. (1999) Rethinking fundamentals of enzyme action. *Advances in enzymology and related areas of molecular biology* 73, 25–56.
- (38) Cornish-Bowden, A. (1984) Enzyme specificity: its meaning in the general case. *J. Theor. Biol.* 108, 451–457.
- (39) Jonna, V. R., Crona, M., Rofougaran, R., Lundin, D., Johansson, S., Brännström, K., Sjöberg, B.-M., and Hofer, A. (2015) Diversity in Overall Activity Regulation of Ribonucleotide Reductase. *J. Biol. Chem.* 290, 17339–17348.
- (40) Chimpoy, K., and Mathews, C. K. (2001) Mouse Ribonucleotide Reductase Control INFLUENCE OF SUBSTRATE BINDING UPON INTERACTIONS WITH ALLOSTERIC EFFECTORS. *J. Biol. Chem.* 276, 7093–7100.
- (41) Larsson, A., and Reichard, P. (1966) Enzymatic synthesis of deoxyribonucleotides X. Reduction of purine ribonucleotides; allosteric behavior and substrate specificity of the enzyme system from *Escherichia coli* B. *J. Biol. Chem.* 241, 2540–2549.
- (42) Eriksson, S., Thelander, L., and Akerman, M. (1979) Allosteric regulation of calf thymus ribonucleoside diphosphate reductase. *Biochemistry* 18, 2948–2952.

(43) Johansson, R., Jonna, V. R., Kumar, R., Nayeri, N., Lundin, D., Sjöberg, B.-M., Hofer, A., and Logan, D. T. (2016) Structural Mechanism of Allosteric Activity Regulation in a Ribonucleotide Reductase with Double ATP Cones. *Structure* 24, 906–917.

(44) Xu, H., Faber, C., Uchiki, T., Fairman, J. W., Racca, J., and Dealwis, C. (2006) Structures of eukaryotic ribonucleotide reductase I provide insights into dNTP regulation. *Proc. Natl. Acad. Sci. U. S. A.* 103, 4022–4027.

(45) Ahmad, M. F., Kaushal, P. S., Wan, Q., Wijerathna, S. R., An, X., Huang, M., and Dealwis, C. G. (2012) Role of arginine 293 and glutamine 288 in communication between catalytic and allosteric sites in yeast ribonucleotide reductase. *J. Mol. Biol.* 419, 315–329.

(46) Ahmad, M. F., and Dealwis, C. G. (2013) The structural basis for the allosteric regulation of ribonucleotide reductase. *Progress in molecular biology and translational science* 117, 389–410.

(47) Xu, H., Faber, C., Uchiki, T., Racca, J., and Dealwis, C. (2006) Structures of eukaryotic ribonucleotide reductase I define gemcitabine diphosphate binding and subunit assembly. *Proc. Natl. Acad. Sci. U. S. A.* 103, 4028–4033.

(48) Kumar, D., Viberg, J., Nilsson, A. K., and Chabes, A. (2010) Highly mutagenic and severely imbalanced dNTP pools can escape detection by the S-phase checkpoint. *Nucleic Acids Res.* 38, 3975–3983.

(49) Kumar, D., Abdulovic, A. L., Viberg, J., Nilsson, A. K., Kunkel, T. A., and Chabes, A. (2011) Mechanisms of mutagenesis in vivo due to imbalanced dNTP pools. *Nucleic Acids Res.* 39, 1360–1371.

(50) Goodey, N. M., and Benkovic, S. J. (2008) Allosteric regulation and catalysis emerge via a common route. *Nat. Chem. Biol.* 4, 474–482.

(51) Tsai, C. J., and Nussinov, R. (2014) A unified view of "how allostery works". *PLoS Comput. Biol.* 10, e1003394.

(52) Carlson, G. M., and Fenton, A. W. (2016) What Mutagenesis Can and Cannot Reveal About Allostery. *Biophys. J.* 110, 1912–1923.

(53) Weinkam, P., Chen, Y. C., Pons, J., and Sali, A. (2013) Impact of mutations on the allosteric conformational equilibrium. *J. Mol. Biol.* 425, 647–661.

(54) Kashlan, O. B., and Cooperman, B. S. (2003) Comprehensive model for allosteric regulation of mammalian ribonucleotide reductase: refinements and consequences. *Biochemistry* 42, 1696–1706.

(55) Hofer, A., Schmidt, P. P., Gråslund, A., and Thelander, L. (1997) Cloning and characterization of the R1 and R2 subunits of ribonucleotide reductase from *Trypanosoma brucei*. *Proc. Natl. Acad. Sci. U. S. A.* 94, 6959–6964.

(56) Nowakowski, S. G., Kolwicz, S. C., Korte, F. S., Luo, Z., Robinson-Hamm, J. N., Page, J. L., Brozovich, F., Weiss, R. S., Tian, R., Murry, C. E., and Regnier, M. (2013) Transgenic overexpression of ribonucleotide reductase improves cardiac performance. *Proc. Natl. Acad. Sci. U. S. A.* 110, 6187–6192.